SEMARAK ILMU PUBLISHING
202103268166(003316878-P)

Journal of Advanced Research in Applied Sciences and Engineering Technology

Journal homepage:
https://semarakilmu.com.my/journals/index.php/applied_sciences_eng_tech/index
ISSN: 2462-1943

Hybrid Conjugate Gradient Backpropagation of GCPV Based DSTATCOM for Power Conditioning

Muhammad Ariff Haikal Ridzwan[1], Nor Hanisah Baharudin[1,2,*], Tunku Muhammad Nizar Tunku Mansur[1,2], Rosnazri Ali[1,2], Mohd Syahril Noor Shah[1]

[1] Faculty of Electrical Engineering & Technology, Universiti Malaysia Perlis, Pauh Putra Campus, 02600 Arau, Perlis, Malaysia
[2] Centre of Excellence for Renewable Energy (CERE), Faculty of Electrical Engineering & Technology, Universiti Malaysia Perlis, Pauh Putra Campus, 02600 Arau, Perlis, Malaysia

ARTICLE INFO

Article history:
Received 30 March 2023
Received in revised form 2 March 2024
Accepted 7 May 2024
Available online 6 June 2024

Keywords:
Backpropagation; PQ Theory; DSTATCOM

ABSTRACT

This paper studies the performance of a hybrid conjugates gradient backpropagation (HCGBP) grid-connected solar photovoltaic (GCPV) based DSTATCOM. This paper proposes a hybrid control algorithm of instantaneous reactive power theory and conjugate gradient backpropagation neural network for an application of a grid-connected solar PV (GCPV) based DSTATCOM for three-phase three-wire system. The fundamental weighted value of active power components of load currents, which is necessary for estimating reference source currents, is extracted using a conjugate gradient backpropagation control algorithm. The performance of the proposed control algorithm has reduced the THD of the line current up to 1.48%. It is proven that HCGBP has better efficiency, faster response and easy to implement. The steady-state performance of the three-phase GCPV-DSTATCOM under non-linear load has been analysed through simulation and Hardware-in-loop (HIL) simulation based on real time DSP system using Texas Instrument TI C2000 32-bit microcontroller in MATLAB/Simulink. Furthermore, the simulation results have shown that the THD of the line current at the PCC has reduced less than 8%, according to the IEEE standard 519:2014.

1. Introduction

Renewable energy sources include wind, solar, geothermal, and others [1]. Renewable energy sources are gaining much attention and support these days, including political motivation and government efforts. Solar photovoltaic system (PV) has become the primary source of electricity generation among sustainable energy resources due to its advantages [2-5]. Solar photovoltaic (PV) system generates electricity directly from solar energy using photovoltaic cells. Photovoltaic energy is derived from the sun's light (photo) to generate a DC voltage (voltaic). When PV cells are exposed to sun irradiations, the electrons in the cells move around, causing an electric current to flow. PV cells are an easy way to generate power because they do not have moving parts, thus require less

* *Corresponding author.*
E-mail address: norhanisahbaharudin@gmail.com

https://doi.org/10.37934/araset.46.2.6480

maintenance, and have a low operational cost compared to other sources of electricity. They also have a long lifespan, do not cause pollution while in use, and can be installed anywhere there is sunlight [6].

The solar photovoltaic (PV) system is then connected to a dc/ac voltage source converter (VSC) in order to supply electricity to the AC utility [3,7]. Because the electricity harnessed from the PV array cannot be supplied directly into the grid and load, a voltage source converter (VSC) that works as a power converter is used. Harmonic currents are injected into the distribution system due to the excessive usage of non-linear loads such as rectifiers. It becomes a major concern for integrating grid-connected solar PV systems to the utility grid [8-10].

Power quality (PQ) problems in the distribution system are the major concern because of the negative impacts on the load's equipment and the utility system [11-13]. Power quality concerns are resolved by implementing VSC as a distribution static compensator (DSTATCOM), which improves the power factor and minimizes harmonics [14]. The performance of DSTATCOMs, on the other hand, is determined by the control algorithm used for the current reference calculation and gating pulse generating scheme. As a result, better convergence, adaptive nature, reduced computing weight, and simple application are essential requirements for developing and implementing a control algorithm. Therefore, the control techniques like Instantaneous Reactive Power (IRP) or P-Q theory, Modified Synchronous Reference Frame Theory (MSRF), Synchronous Reference Frame Theory (SRF), Average Unit Power Factor theory (AUPF) and Instantaneous Symmetrical Control theory, are commonly being used to control the DSTATCOM [15,16].

As a result, better concentration and adaptive nature are essential requirements to develop and implement control algorithms while reducing the weight of computing and simple applications. For various applications, neural network (NN) control algorithms are used due to their combinational neural structure and improved accuracy. Hence, neural network-based control techniques are increasingly used for quick harmonic analysis and detection. The main benefits of this technique are greater reliability, energy efficient and improved performance without requiring significant hardware changes. Furthermore, while dealing with power quality issues, the gradient descent with momentum NN-based control technique is capable of reducing uncertainties, nonlinearities, and harmonics, resulting in an appropriate response [8].

In this study, an HCGBP method is developed in a three-phase DSTATCOM to extract the weighted value of non-linear load active power current components. It is slow throughout the training process because of the increased number of learning steps, but this algorithm gives a very quick trained output response after weight training. The proposed control technique on a DSTATCOM is utilized in this application to compensate the non-linear load and boost the performance of Instantaneous reactive power theory.

2. DSTATCOM Topology

DSTATCOM can be categorized into two types: Current Source Converter (CSC) and Voltage Source Converter (VSC). VSC is a more widespread application than CSC for its advantages of having self-supporting DC bus voltage through a DC bus capacitor. Moreover, VSC also holds other benefits such as low cost, lighter, and the installation can be expanded into multilevel form to improve the lower switching frequency performance [17].

DSTATCOM can be used according to its application in the distribution system. The distribution systems are frequently in three-phase. Thus, DTATCOMs can be in three-phase three-wire (3P3W) or three-phase four-wire (3P4W), depending on the different kinds of loads. Therefore, DSTATCOM is categorized according to the needs of consumer load in the distribution system, i.e., single-phase load, three-phase load, and a combination of single-phase and three-phase loads. Single-phase loads are usually like TVs, air conditioners, laser printers, and ovens, which may disrupt the power quality. Besides, the three-phase load is the largest user of AC power as most industries use three-phase loads, such as arc furnaces and traction loads [17] .

2.1 PV-DSTATCOM

A Photovoltaic (PV) system is one of the sources of distribution generation (DG) used as a reliable source for the utility grid to fulfil the customer's demand. The grid-connected PV system interfacing with DSTATCOM can benefit PQ improvement and transfer the PV source energy to the load and the remaining energy to the utility grid. The performance of PV-DSTATCOM varies depend on the presence of sunlight. During daylight, the VSC performs a dual function of improving the power quality as a DSTATCOM and feeds power supply from the PV array to the load and the utility grid. At night, when the sunlight is absent, the VSC will act as a DSTATCOM and maintain the task of improving the power quality with the power transfer from the utility grid to the load [2,18,19].

The topologies of the inverter in the DSTATCOM can be classified into two categories when interfacing with a PV system: single-stage inverter (SSI) and multiple-stage inverter (MSI). Figure 1 shows the configuration Single-Stage Inverter Based 3P3W PV-DSTATCOM. The SSI conduct all tasks, including DSTATCOM control and MPPT [20].

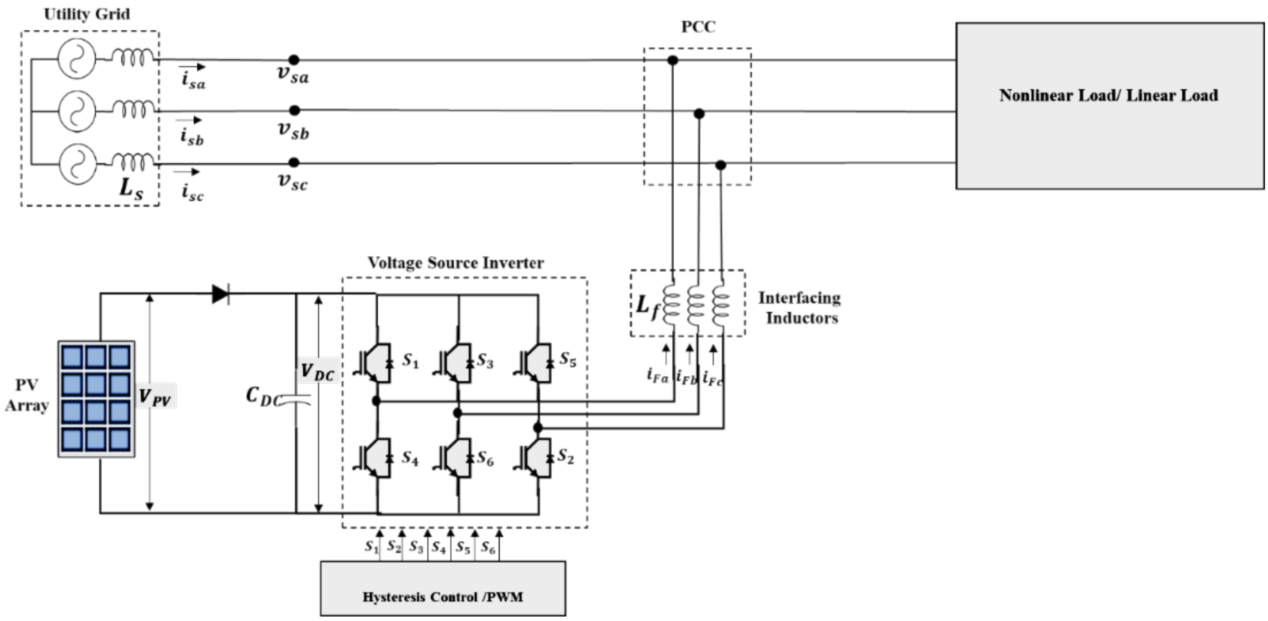

Fig. 1. Single-Stage Inverter Based 3P3W PV-DSTATCOM [22]

In SSI, the PV panel in the PV generator is connected directly to the dc side of VSC. The double-stage inverter is an example of MSI illustrated in Figure 2. The double-stage inverter, or VSC, consists of a two-stage PV separated by the MPPT and DSTATCOM. According to Figure 2, the first stage is a dc-dc boost converter. The first stage is in charge of obtaining the maximum power from the Solar PV array. First, the small capacitor connects the PV panel to the boost converter's input side. Then, the boost converter is connected to the dc side of the VSC. The second stage is the VSC. The VSC acts as DSTATCOM and feed the utility grid and the non-linear load through the point of common coupling (PCC), as illustrated in Figure 2 [21].

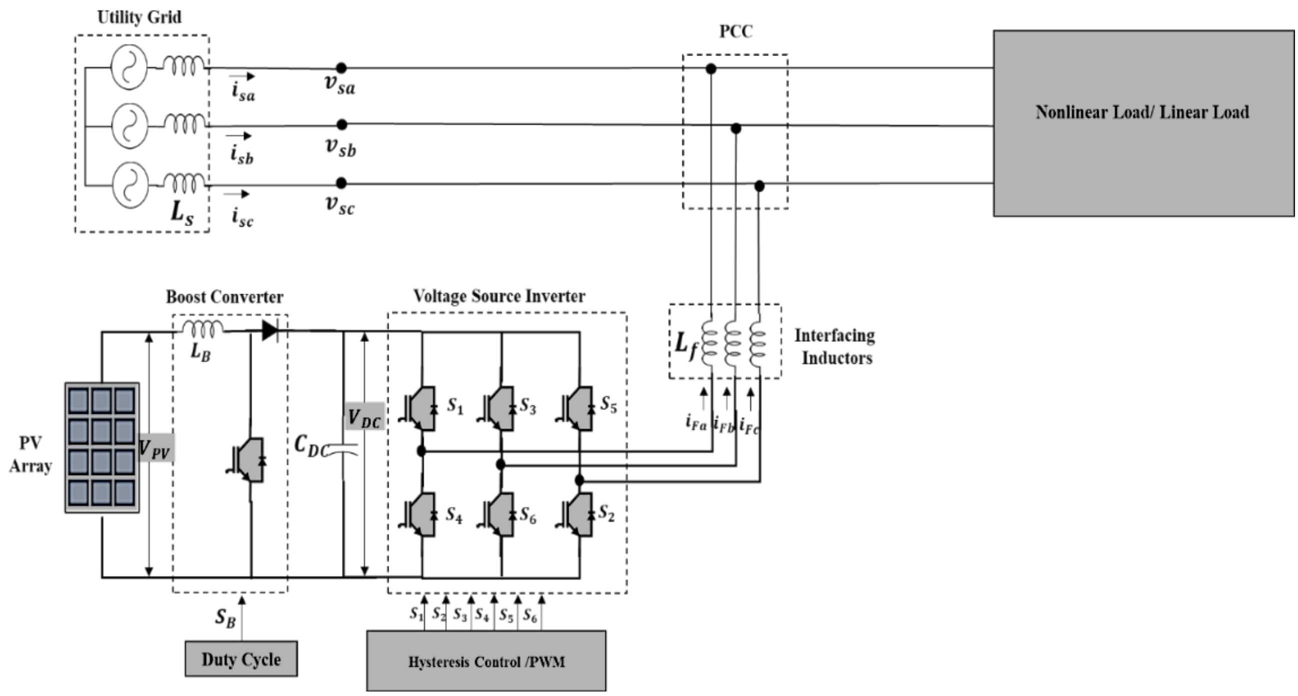

Fig. 2. Double-Stage Inverter Based 3P3W PV-DSTATCOM [21]

3. Control Algorithm

To avoid significant PQ problems, the control algorithm is critical to DSTATCOM's efficiency in producing reference current signals. Different control strategies, such as Instantaneous Reactive Power (IRP) theory or P-Q theory, Synchronous references frame (SRF) theory, Discrete Fourier transform (DFT), and wavelet transform, are available for generating reference current signals. P-Q theory is the most effective control algorithm for resolving PQ problems. A dc voltage regulator is used to maintain the DSTATCOM DC-link voltage [23].

H. Akagi *et al.,* introduced the Instantaneous Reactive Power theory for inner loop control in shunt active filters in 1984 [24]. On the other hand, the fundamental disadvantage of this approach is that the control algorithm's performance is inadequate when the grid voltage is imbalanced and distorted [25-27]. A phase-locked loop system, a d-q transformation, and computations for the inverse d-q transformation are required for the Synchronous Reference Frame approach to inner loop control [28]. A PI control algorithm can control the DC-link voltage for power flow control and power balancing in an active shunt filter. Besides, the adaptive fuzzy logic control algorithm is an alternative method for the outer loop control of active shunt filters that provides better dynamic performance and adapts to changes in system parameters [29,30].

Instantaneous Reactive Power theory has considerably improved the performance of a distribution static compensator (DSTATCOM) [31]. The PV-DSTATCOM combination, on the other hand, has just recently been established over several years [32]. This system can simultaneously improve power factor, current imbalance, and current harmonics, as well as inject solar PV energy with low total harmonic distortion (THD). When no electricity is generated by the GCPV, the system can enhance the utility's power quality. Towards the finest of our knowledge, Kim *et al.,* first introduced this concept in 1996 [3,33].

3.1 Instantaneous Reactive Power Theory

The control algorithm Instantaneous Reactive Power (IRP) theory or P-Q Theory proposed by Akagi is also known as P-Q theory. The P-Q theory will convert the acquired three-phase line voltage and load currents into two-phase quantities in the $\alpha\beta$ frame using Clark's transformation. In this frame, P-Q theory also integrates active and reactive power. Using reverse Clark's transformation, the *abc* frame are converted from the reference currents in the $\alpha\beta$ frame. Clark's transformation also converted the line voltages (*V_a, V_b, and V_c*) as well as the load to current (*I_{La}, I_{Lb}, and I_{Lc}*) into $\alpha\beta$ frame as in Eq. (1) and Eq. (2) [27,34].

$$\begin{bmatrix} V_\alpha \\ V_\beta \end{bmatrix} = \sqrt{\frac{2}{3}} \begin{bmatrix} 1 & -1/2 & -1/2 \\ 0 & \sqrt{3}/2 & -\sqrt{3}/2 \end{bmatrix} \begin{bmatrix} V_a \\ V_b \\ V_c \end{bmatrix} \tag{1}$$

$$\begin{bmatrix} I_\alpha \\ I_\beta \end{bmatrix} = \sqrt{\frac{2}{3}} \begin{bmatrix} 1 & -1/2 & -1/2 \\ 0 & \sqrt{3}/2 & -\sqrt{3}/2 \end{bmatrix} \begin{bmatrix} I_{La} \\ I_{Lb} \\ I_{Lc} \end{bmatrix} \tag{2}$$

The instantaneous active and reactive powers can be generated are as follows:

$$\begin{bmatrix} p \\ q \end{bmatrix} = \begin{bmatrix} V_\alpha & V_\beta \\ -V_\beta & V_\alpha \end{bmatrix} \begin{bmatrix} I_\alpha \\ I_\beta \end{bmatrix} \tag{3}$$

Average $(\bar{p})$ and oscillatory $(\tilde{p})$ are the results of instantaneous active and reactive power p and q after being decomposed. The reference source currents are used to correct the oscillatory component of instantaneous active power. I_α^* and I_β^* are calculated based on the following equation:

$$\begin{bmatrix} I_\alpha^* \\ I_\beta^* \end{bmatrix} = \frac{1}{\Delta} \begin{bmatrix} V_\alpha & -V_\alpha \\ V_\beta & V_\beta \end{bmatrix} \begin{bmatrix} \bar{P} \\ 0 \end{bmatrix} \tag{4}$$

Where $\Delta = V_\alpha^2 + V_\beta^2$ .The reverse Clark's transformation is used to generate reference source currents in the *abc* frame by using reference source currents in the $\alpha\beta$ frame as shown in Eq. (5).

$$\begin{bmatrix} I_a^* \\ I_b^* \\ I_c^* \end{bmatrix} = \sqrt{\frac{2}{3}} \begin{bmatrix} 1/\sqrt{2} & 1 & 0 \\ 1/\sqrt{2} & -1/2 & \sqrt{3}/2 \\ 1/\sqrt{2} & -1/2 & -\sqrt{3}/2 \end{bmatrix} \begin{bmatrix} I_0^* \\ I_\alpha^* \\ I_\beta^* \end{bmatrix} \tag{5}$$

3.2 Neural Network Configuration

In order to improve the performance of DSTATCOM, hybrid conjugate gradient backpropagation (HCGBP) neural network-based P-Q theory control algorithm is proposed in this paper. Figure 3 shows the proposed neural network-based P-Q theory block diagram for three-phase three-wire DSTATCOM. To increase P-Q performance, the calculated *P* will be filtered and generated by a neural network in NN1. This also be applied to calculated P_{DC}, which will be filtered and generated by the neural network in NN2 [35]. The generated $\bar{P}$ and P_{DC} by the neural network will be used to estimate the current reference. Then, the estimated current reference will be used in the hysteresis control.

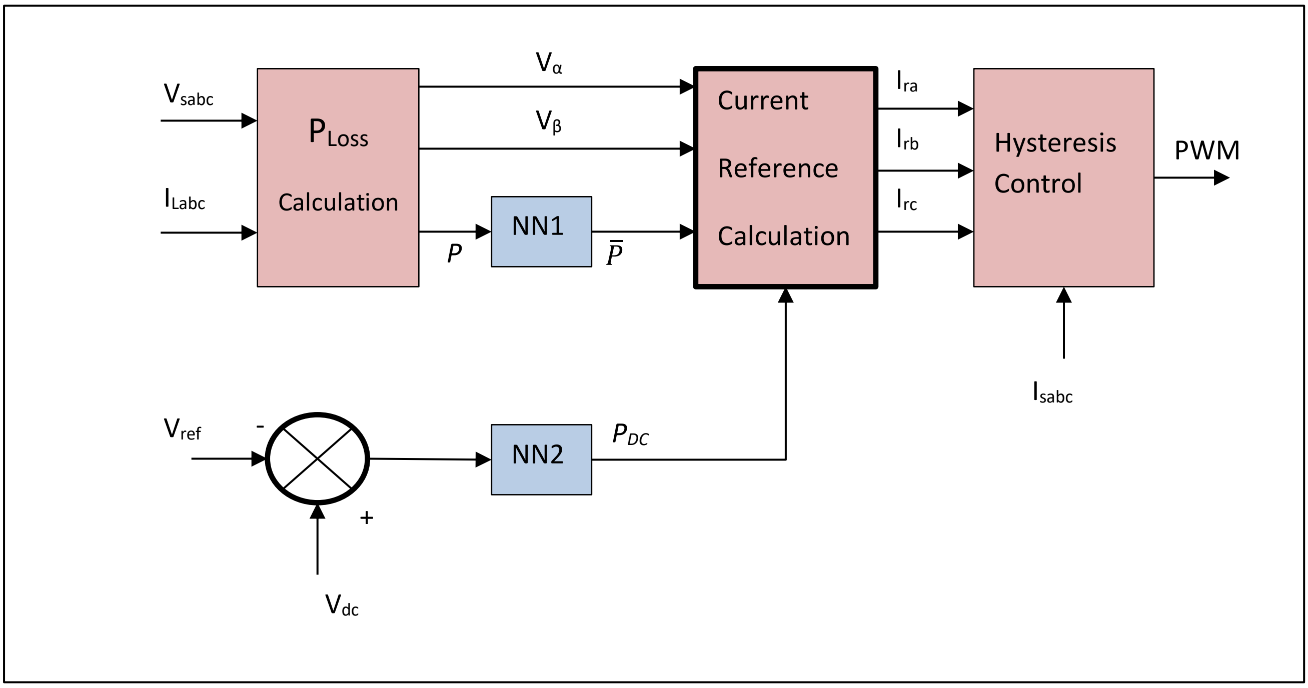

Fig. 3. Block diagram of the proposed HCGBP control algorithm for 3P3W DSTATCOM

Table 1 shows the neural network training parameters in MATLAB, there are three layers that are represented as input layer with one input neuron, a hidden layer with 10 hidden neurons, and an output layer with a single output neuron. The training part of the neural network occurs in hidden layers. The hidden layer is a bit arbitrary, and 10 hidden neurons are chosen for better performance of the system [36]. The number of hidden layers and the neuron in each layer depend on the problem's complexity [37]. The number of input and output layers for the ANN is constrained by the number of inputs and outputs of the problem. The number of the hidden layer is designed according to the problem. The optimum number of neurons in the hidden layer can be chosen based on the training time and the neural network's performance based on mean squared error (MSE). The number of hidden layers can be changed based on the problem data in the training process.

Table 1
Neural Networks Training Parameters in MATLAB

Parameter	Value	
	NN1	NN2
No. of Training Data	700	700
No of Testing data	150	150
No of neurons in input layer	1	1
No of neurons in hidden layer	10	10
Training Function	Scaled Conjugate Gradient	Scaled Conjugate Gradient
Performance Function	Mean Squared Error (MSE)	Mean Squared Error (MSE)
Maximum epoch	1000	1000

4. Result and Discussion

The proposed control that has been designed using MATLAB/Simulink is discussed in this section. The simulation results will be recorded under non-linear load steady-state condition. The results are presented based on simulation obtained in MATLAB/Simulink.

4.1 Steady-State Performance of GCPV-DSTATCOM using P-Q Control Algorithm Under Non-Linear Load

Figure 4 and Figure 5 show the performance of the developed three-phase three-wire grid-connected photovoltaic with DSTATCOM (GCPV-DSTATCOM) based P-Q theory under non-linear load. Figure 4 (a) shows the waveform analysis for Line Current, Load Current, and Compensation Current. In contrast, Figure 4 (b) shows the waveform analysis for Line Voltage, Load Voltage, and DC-link Voltage (V_{dc}). Figure 4 (a) shows the waveform generated by line current is in sinewave, while load current generates a distorted waveform.

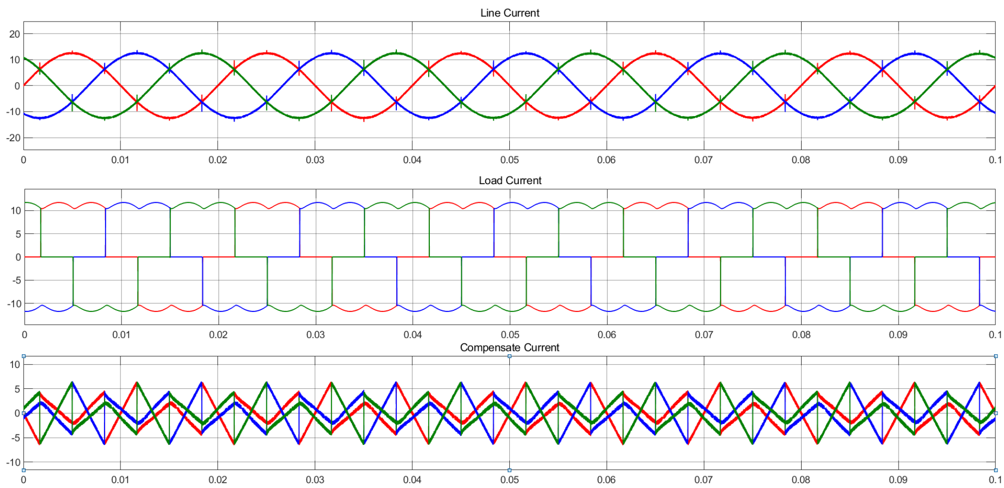

(a)

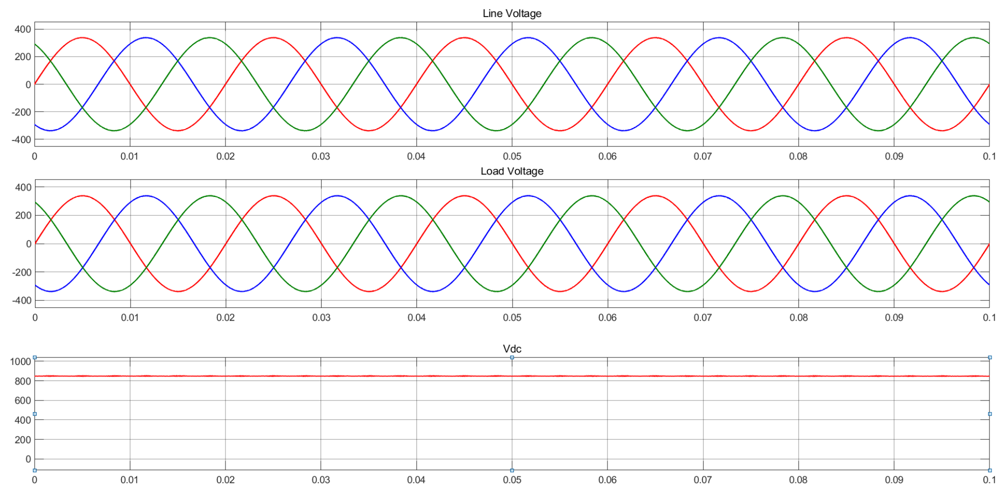

(b)

Fig. 4. Waveform analysis of three-phase three-wire GCPV-DSTATCOM based P-Q theory control algorithm under non-linear load in steady-state condition (a) line current, load current, and compensation current, and (b) line voltage, load voltage, and dc-link voltage

Figure 5 shows the FFT analysis for GCPV-DSTATCOM under non-linear load steady-state condition.

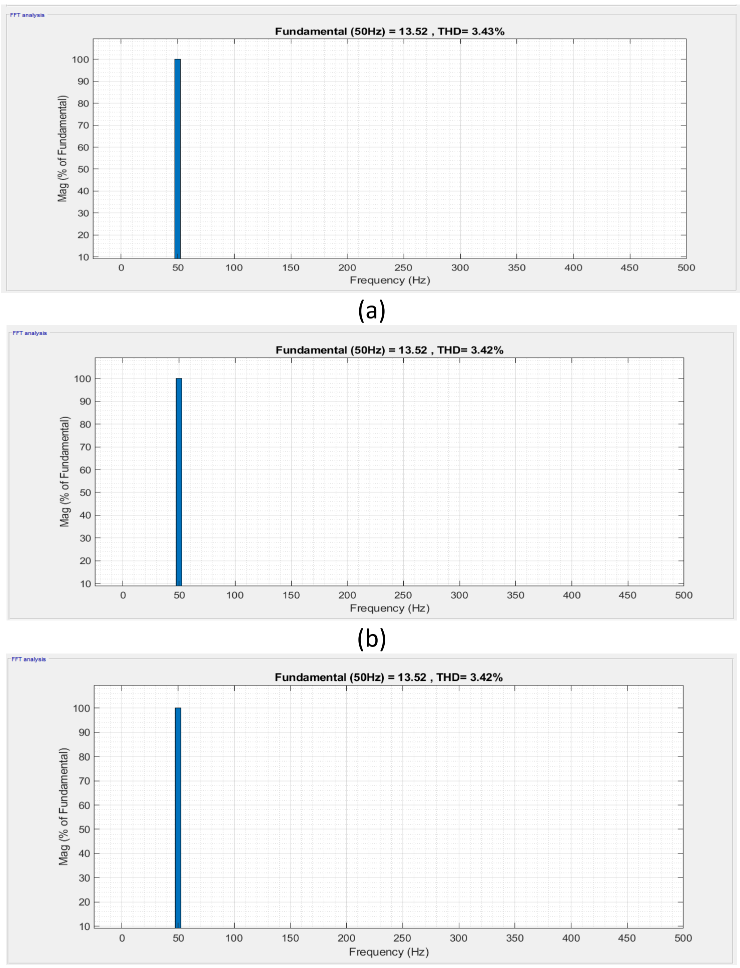

Fig. 5. FFT Analysis of line current (a) Phase A, (b) Phase B, (c) Phase C

Table 2 shows the value THD of the line current is 3.43%, 3.42%, and 3.42%, respectively, for Phase A, B, and C. As a result, the THD of line current has followed the IEEE-519:2014 standard limit which is less than 8%. It is observed that the PQ-based-DSTATCOM is capable of performing harmonic elimination functions.

Table 2
Comparison THD analysis for GCPV-DSTATCOM using P-Q control algorithm and HCGBP control algorithm under non-linear load in steady-state conditions

Phase	THD (%) using P-Q control algorithm		THD (%) using HCGBP control algorithm	
	Line Current	Load Current	Line Current	Load Current
Phase A	3.43	30.64	1.49	30.62
Phase B	3.42	30.63	1.50	30.65
Phase C	3.42	30.63	1.48	30.63

4.2 Steady-State Performance of GCPV-DSTATCOM using HCGBP Control Algorithm under Non-Linear Load

Figure 6 and Figure 7 show the results recorded during the MATLAB simulation. Figure 6 (a) consists of line current, load current, and compensation current, while Figure 6 (b) consists of line voltage, load voltage, and dc-link voltage (V_{dc}). Figure 6 (a) shows that the line current waveforms are in sinewave, while the load current is distorted waveforms.

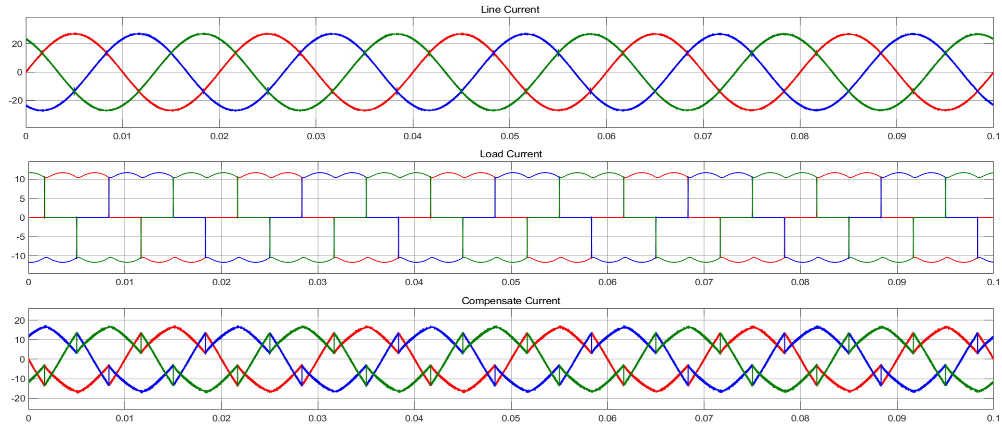

(a)

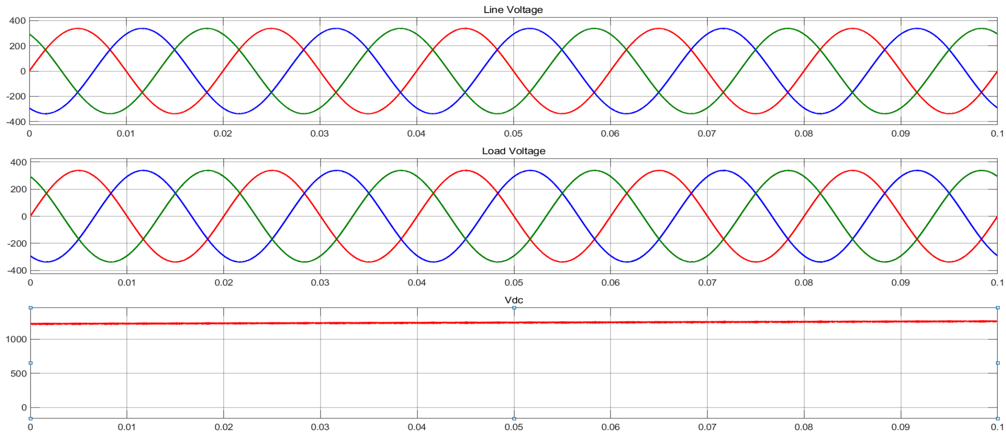

(b)

Fig. 6. Waveform analysis of three-phase three-wire GCPV-DSTATCOM based HCGBP control algorithm under non-linear load (a) line current, load current, and compensation current, (b) line voltage, load voltage, and dc-link voltage

Figure 7 shows the FFT analysis for GCPV-DSTATCOM under non-linear load steady-state condition.

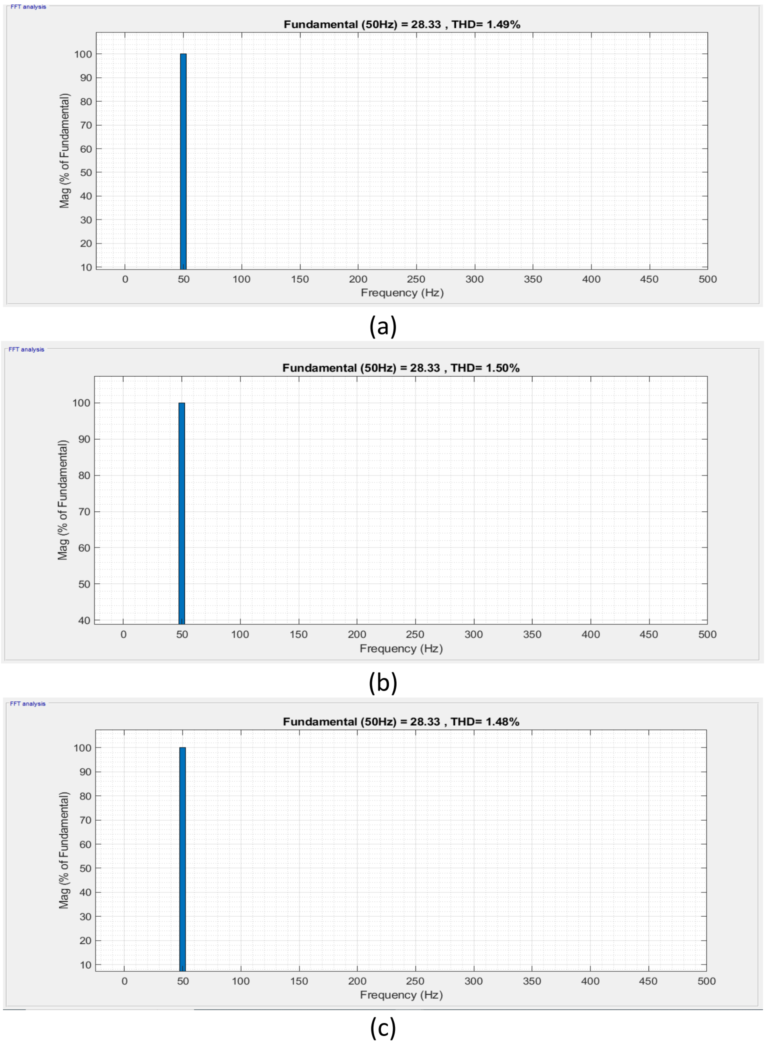

Fig. 7. FFT Analysis for line current (a) Phase A, (b) Phase B, and (c) Phase C

Table 3 shows that the THD of line currents are 1.49%, 1.50%, and 1.48%, respectively, for Phases A, B, and C. As a result, the THD of line current has followed the IEEE-519:2014 standard limit of less than 8% at the PCC. It is discovered that the HCGBP control algorithm for GCPV-DSTATCOM is also capable of performing harmonic elimination functions.

Table 3
Comparison of THD Analysis for GCPV-DSTATCOM using P-Q and HCGBP Control Algorithm under non-linear load steady-state conditions

Phase	THD (%) using PQ control algorithm		THD (%) using HCGBP control algorithm	
	Line Current	Load Current	Line Current	Load Current
Phase A	3.70	25.28	2.64	25.14
Phase B	3.86	25.12	2.65	25.36
Phase C	3.77	25.29	2.71	25.31

Table 4 shows the comparison between P-Q and HCGBP control algorithms. It has been observed that HCGBP can boost the performance of P-Q control algorithm because HCGBP can reduce the THD of the line currents up to 1.48% as compared to the conventional P-Q control algorithm only can reduce THD up to 3.42%.

Table 4
Comparison of Different Control Algorithm for DSTATCOM

Table THD (%)	Control Algorithm					
	P-Q Theory	HCGBP	SRF [38]	FONF[39]	UPQC[40]	LDLMS[41]
Line Current	3.42	1.48	3.33	1.88	2.4	1.94
Load Current	30.63	30.63	26.65	27.66	28.8	21.66

4.3 Steady-State Performance of Hardware-in-the-Loop (HIL) Simulation for GCPV-DSTATCOM using P-Q Control Algorithm under Non-Linear Load.

Figure 8 and Figure 9 show the results recorded during Hardware-in-loop (HIL) simulation based on real time DSP system using Texas Instrument TI C2000 32-bit microcontroller. Figure 8 (a) consists of line current, load current, and compensation current, while Figure 8 (b) consists of line voltage, load voltage, and dc-link voltage (V_{dc}). Figure 8 (a) shows the line currents waveforms are in sinewave, while the load currents are distorted waveforms.

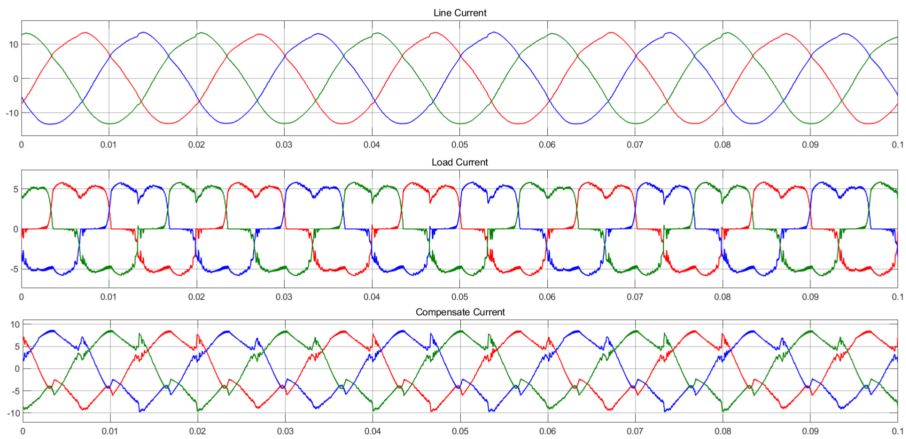

(a)

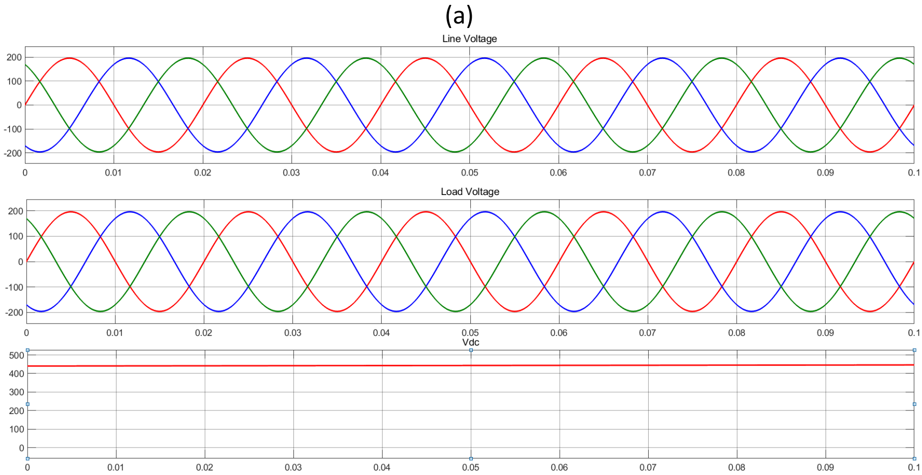

(b)

Fig. 8. Waveform analysis for HIL simulation of three-phase three-wire GCPV-DSTATCOM based P-Q control algorithm under non-linear load steady-state

condition (a) line current, load current, and compensation current (b) line voltage, load voltage, and dc-link voltage

Figure 9 shows the FFT analysis for GCPV-DSTATCOM under non-linear load steady-state conditions. The result shows the THD of line currents are 3.70%, 3.86% and 3.77%, respectively, for phase A, B and C. As a result, the THD of line current for phases A, B and C well within the IEEE-519:2014 standard limit of less than 8% for line current. This shows the P-Q theory can mitigate and reduce harmonics in a hardware simulation environment, as showed by the low THD values for line current which is within the specified limits set by the IEEE-519:2014 standards.

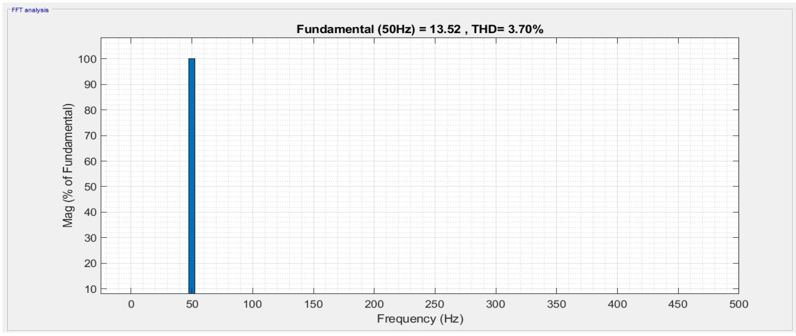

(a)

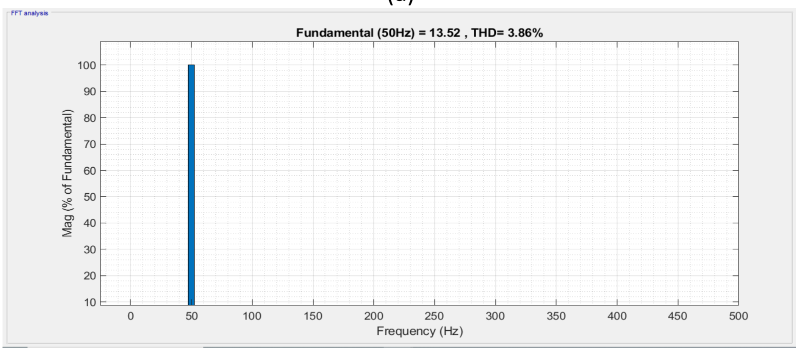

(b)

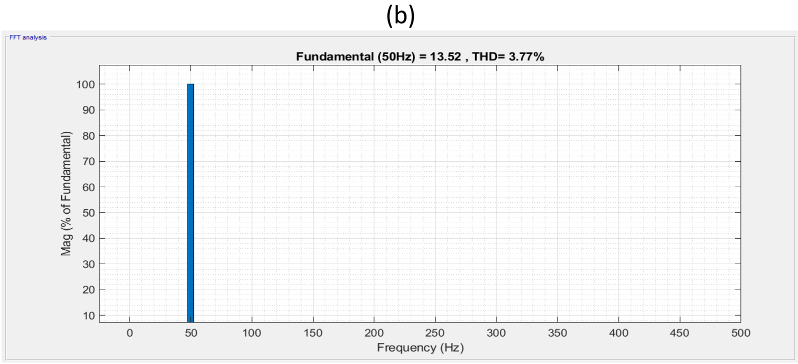

(c)

Fig. 9. FFT analysis for line current (a) Phase A, (b) Phase B, and (c) Phase C

4.4 Steady-State Performance of Hardware-in-the-Loop (HIL) Simulation for GCPV-DSTATCOM using HCGBP Control Algorithm under Non-Linear Load.

Figure 10 and Figure 11 show the result that has been recorded during the HIL simulation. Figure 10 (a) consists of line current, load current, and compensation current, while Figure 10 (b) consists of line voltage, load voltage, and dc-link voltage (V_{dc}). Figure 10 (a) shows that the waveforms generated by the line current are in sinewave, while the load currents are distorted waveforms.

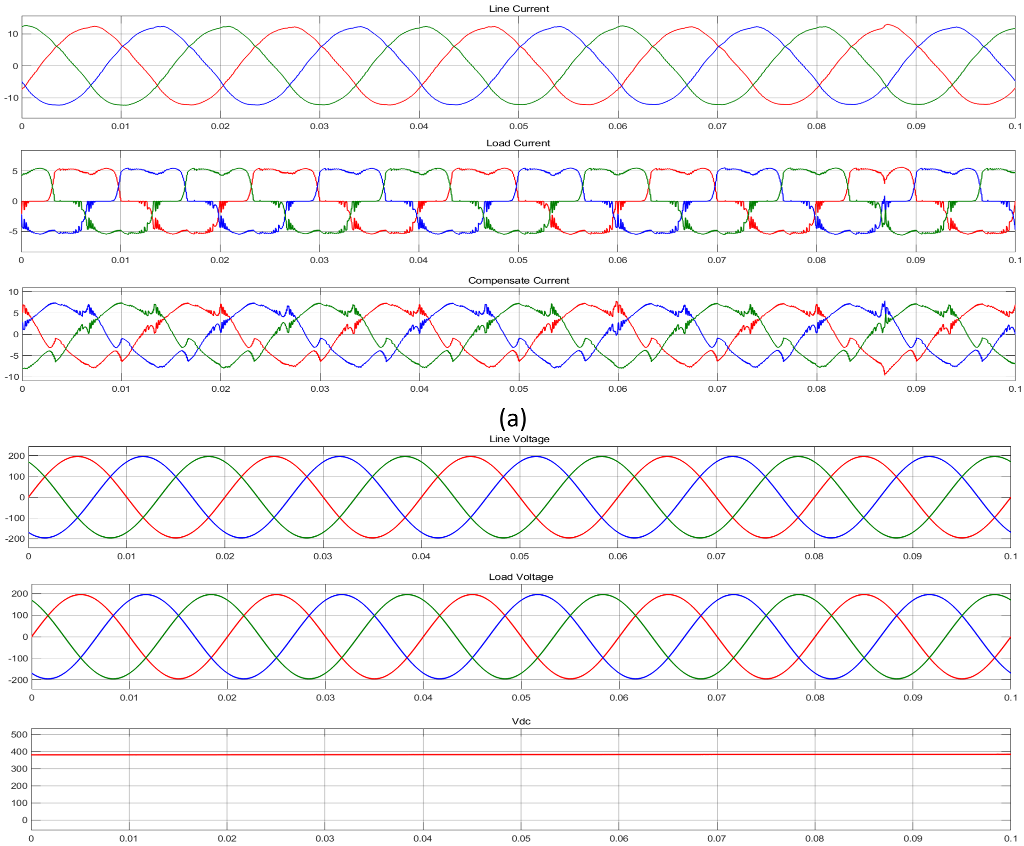

(a)

(b)

Fig. 10. Waveform analysis for HIL simulation of three-phase three-wire GCPV-DSTATCOM based HCGBP control algorithm under linear load steady-state condition (a) line current, load current, and compensation current (b) line voltage, load voltage, and dc-link voltage

Figure 11 shows the FFT analysis for GCPV-DSTATCOM under non-linear load steady-state condition. The results present the value THD of Line current are 2.64%, 2.65%, and 2.71%, respectively, for phases A, B, and C. As a result, the THD of line currents have followed the IEEE-519:2014 standard limit of less than 8% at the PCC. These results demonstrate that the HCGBP control algorithm can be utilized in a real-time hardware experimental platform for harmonic current elimination.

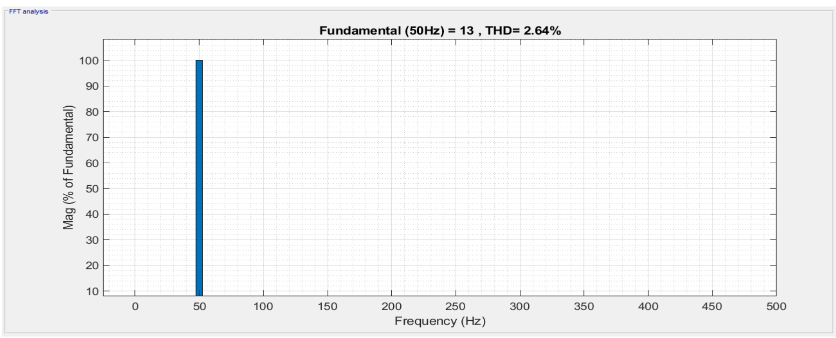

(a)

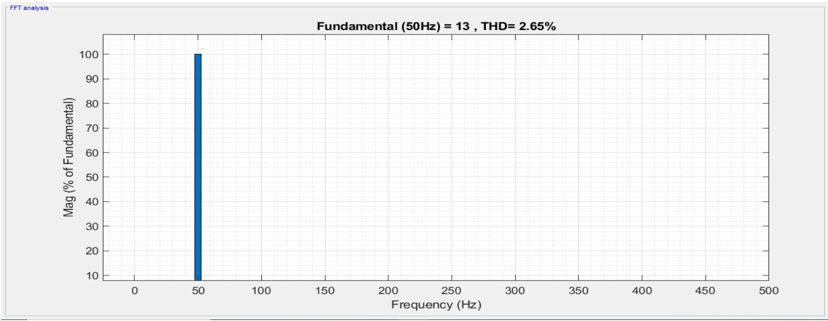

(b)

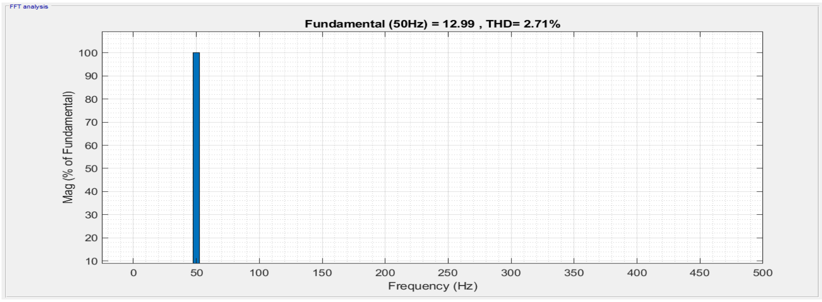

(c)

Fig. 11. FFT analysis for line current (a) Phase A, (b) Phase B, and (c) Phase C

5. Conclusion

The increased use of non-linear loads has caused harmonic distortions and power quality disturbances in power system. DSTATCOM is one of the significant methods for reducing harmonic currents in the distribution system. This paper demonstrates the proposed GCPV-DSTATCOM system with Hybrid Conjugate Gradient Backpropagation Neural Network (HCGBP) control algorithm with Instantaneous Reactive Power (P-Q) theory. The proposed HCGBP control algorithm was utilized to extract reference source currents and generate the switching pulses for the VSC-based DSTATCOM. To demonstrate its effectiveness, a three-phase three-wire GCPV-DSTATCOM with a HCGBP control algorithm was used to compensate the non-linear load compared to conventional P-Q theory in simulation and HIL simulation. According to the simulation results, the proposed GCPV-DSTATCOM system with Hybrid Conjugate Gradient Backpropagation Neural Network (HCGBP) control algorithm can eliminate harmonic currents and improve the THD value of line currents in accordance with the IEEE-519:2014 standard at the PCC. Based on the observations, the proposed Hybrid Conjugate Gradient Backpropagation Neural Network (HCGBP) control algorithm can also improve the performance of the conventional P-Q theory control algorithm up to 15.83% in HIL simulation.

Acknowledgement
The author would like to acknowledge the support from the Fundamental Research Grant Scheme (FRGS) under a grant number of FRGS/1/2020/TK0/UNIMAP/02/113 from the Ministry of Education Malaysia.

References

[1] Dongare, Mandar, and Manohar Kalgunde. "Mitigation of lower order harmonics in a grid-connected single-phase PV inverter using shunt active filter." In *2017 International Conference on Current Trends in Computer,*

Electrical, Electronics and Communication (CTCEEC), pp. 192-197. IEEE, 2017. https://doi.org/10.1109/CTCEEC.2017.8455001

[2] Mansur, T. M. N. T., N. H. Baharudin, and R. Ali. "Design of 4. 0 kWp Solar PV System for Residential House under Net Energy Metering Scheme." *J. Eng. Res. Educ* 9 (2017): 95-106.

[3] Tuyen, Nguyen Duc, and Goro Fujita. "PV-active power filter combination supplies power to nonlinear load and compensates utility current." *IEEE Power and Energy Technology Systems Journal* 2, no. 1 (2015): 32-42. https://doi.org/10.1109/JPETS.2015.2404355

[4] Jain, Vandana, and Bhim Singh. "Power quality improvement in PV system tied to weak grid." *IEEE Transactions on Industry Applications* 57, no. 2 (2020): 1265-1273. https://doi.org/10.1109/TIA.2020.3045961

[5] Chakraborty, Subhadip, Gaurav Modi, and Bhim Singh. "An EAFOGI-FLL Based Adaptive Control for Seamless Operation of a Solar Photovoltaic System." In *2022 IEEE Industry Applications Society Annual Meeting (IAS)*, pp. 1-6. IEEE, 2022. https://doi.org/10.1109/TIA.2022.3191210

[6] Taha, Amna Babikir, and Sharief Fadul Babiker. "Irradiance Variation Effect on the Electrical Performance of a Grid Connected PV System." In *2019 International Conference on Computer, Control, Electrical, and Electronics Engineering (ICCCEEE)*, pp. 1-4. IEEE, 2019. https://doi.org/10.1109/ICCCEEE46830.2019.9071427

[7] Chatterjee, Aditi, and Kanungo Barada Mohanty. "Current control strategies for single phase grid integrated inverters for photovoltaic applications-a review." *Renewable and Sustainable Energy Reviews* 92 (2018): 554-569. https://doi.org/10.1016/j.rser.2018.04.115

[8] Shukl, Pavitra, and Bhim Singh. "Neural network based control algorithm for solar PV interfaced system." In *2019 IEEE Energy Conversion Congress and Exposition (ECCE)*, pp. 2552-2559. IEEE, 2019. https://doi.org/10.1109/ECCE.2019.8912238

[9] Liang, Xiaodong. "Emerging power quality challenges due to integration of renewable energy sources." *IEEE Transactions on Industry Applications* 53, no. 2 (2016): 855-866. https://doi.org/10.1109/TIA.2016.2626253

[10] Nwaigwe, K. N., Philemon Mutabilwa, and Edward Dintwa. "An overview of solar power (PV systems) integration into electricity grids." *Materials Science for Energy Technologies* 2, no. 3 (2019): 629-633. https://doi.org/10.1016/j.mset.2019.07.002

[11] Devassy, Sachin, and Bhim Singh. "Modified pq-theory-based control of solar-PV-integrated UPQC-S." *IEEE Transactions on Industry Applications* 53, no. 5 (2017): 5031-5040. https://doi.org/10.1109/TIA.2017.2714138

[12] Belaidi, Rachid, Ali Haddouche, Djamila Ghribi, and M. Mghezzi Larafi. "A Three-Phase Grid-Connected PV System Based on SAPF for Power Quality Improvement." *TELKOMNIKA (Telecommunication Computing Electronics and Control)* 15, no. 3 (2017): 1003-1011. https://doi.org/10.12928/telkomnika.v15i3.5439

[13] Kumar, Rajat, Raj Kumar, Sanjay Marwaha, and Bhim Singh. "S-Transform Based Detection of Multiple and Multistage Power Quality Disturbances." In *2020 IEEE 9th Power India International Conference (PIICON)*, pp. 1-5. IEEE, 2020. https://doi.org/10.1109/PIICON49524.2020.9112945

[14] Kandpal, Bakul, K. P. Tomar, Ikhlaq Hussain, and Bhim Singh. "Adaptive control of a grid-connected SPV system with DSTATCOM capabilities." In *2017 4th IEEE Uttar Pradesh Section International Conference on Electrical, Computer and Electronics (UPCON)*, pp. 452-456. IEEE, 2017. https://doi.org/10.1109/UPCON.2017.8251090

[15] Sheila, H., and Shobha Shankar. "Study of Power Quality Issues in Wind Distributed Generation System." In *2017 International Conference on Current Trends in Computer, Electrical, Electronics and Communication (CTCEEC)*, pp. 664-668. IEEE, 2017.

[16] Koduri, Omkar, SSSR Sarathbabu Duvvuri, and Sagiraju Dileep Kumar Varma. "A novel passive islanding detection methods using wavelet transform for Grid Connected PV System." In *2018 IEEE 13th International Conference on Industrial and Information Systems (ICIIS)*, pp. 422-426. IEEE, 2018. https://doi.org/10.1109/ICIINFS.2018.8721382

[17] Singh, Bhim, Ambrish Chandra, and Kamal Al-Haddad. *Power quality: problems and mitigation techniques*. John Wiley & Sons, 2014. https://doi.org/10.1002/9781118922064

[18] Singh, Bhim, and Vandana Jain. "TOCF based control for optimum operation of a grid tied solar PV system." *IEEE Transactions on Energy Conversion* 35, no. 3 (2020): 1171-1181. https://doi.org/10.1109/TEC.2020.2990907

[19] Mansur, T. M. N. T., N. H. Baharudin, and R. Ali. "A comparative study for different sizing of solar PV system under net energy metering scheme at university buildings." *Bulletin of Electrical Engineering and Informatics* 7, no. 3 (2018): 450-457. https://doi.org/10.11591/eei.v7i3.1277

[20] Kjaer, Soeren Baekhoej, John K. Pedersen, and Frede Blaabjerg. "A review of single-phase grid-connected inverters for photovoltaic modules." *IEEE transactions on industry applications* 41, no. 5 (2005): 1292-1306. https://doi.org/10.1109/TIA.2005.853371

[21] Modi, Gaurav, Shailendra Kumar, and Bhim Singh. "Improved Widrow–Hoff based adaptive control of multiobjective PV-DSTATCOM system." *IEEE Transactions on Industry Applications* 56, no. 2 (2019): 1930-1939. https://doi.org/10.1109/TIA.2019.2960732

[22] Jain, Vandana, Ikhlaq Hussain, and Bhim Singh. "A HTF-based higher-order adaptive control of single-stage grid-interfaced PV system." *IEEE Transactions on Industry Applications* 55, no. 2 (2018): 1873-1881. https://doi.org/10.1109/TIA.2018.2878186

[23] Murali, M. R. V., K. Srinivasu, and LV Narasimha Rao. "Enhancement of Power Quality with ANFIS controlled DSTATCOM in four wire three phase distribution system." In *2016 Biennial International Conference on Power and Energy Systems: Towards Sustainable Energy (PESTSE)*, pp. 1-8. IEEE, 2016. https://doi.org/10.1109/PESTSE.2016.7516416

[24] Akagi, Hirofumi, Yoshihira Kanazawa, and Akira Nabae. "Instantaneous reactive power compensators comprising switching devices without energy storage components." *IEEE Transactions on industry applications* 3 (1984): 625-630. https://doi.org/10.1109/TIA.1984.4504460

[25] Katole, D. N., M. B. Daigavane, S. P. Gawande, and P. M. Daigavane. "Improved single phase instantaneous pq theory for DVR compensating nonlinear load." In *2018 IEEE International Conference on Power Electronics, Drives and Energy Systems (PEDES)*, pp. 1-6. IEEE, 2018. https://doi.org/10.1109/PEDES.2018.8707479

[26] Benedicte, Manishimwe, and Peter Musau Moses. "Design of Hybrid Active Power Filters (HAPFs) for Grid-Connected Photovoltaic Systems Using Modified pq theory." In *2022 IEEE PES/IAS PowerAfrica*, pp. 1-5. IEEE, 2022. https://doi.org/10.1109/PowerAfrica53997.2022.9905402

[27] Sanjan, P. S., N. G. Yamini, and N. Gowtham. "Performance comparison of single-phase SAPF using PQ theory and SRF theory." In *2020 international conference for emerging technology (INCET)*, pp. 1-6. IEEE, 2020. https://doi.org/10.1109/INCET49848.2020.9154126

[28] Bhattacharya, Subhashish, and Deepak Divan. "Design and implementation of a hybrid series active filter system." In *Proceedings of PESC'95-Power Electronics Specialist Conference*, vol. 1, pp. 189-195. IEEE, 1995.

[29] Akagi, Hirofumi. "The state-of-the-art of active filters for power conditioning." In *2005 European Conference on Power Electronics and Applications*, pp. 15-pp. IEEE, 2005. https://doi.org/10.1109/EPE.2005.219768

[30] Jayasankar, V. N., and U. Vinatha. "Modified instantaneous power theory and fuzzy logic based controller for grid-connected hybrid renewable energy system with shunt active power filter functionality." (2019).

[31] Peng, Fang Zheng, and Jih-Sheng Lai. "Generalized instantaneous reactive power theory for three-phase power systems." *IEEE transactions on instrumentation and measurement* 45, no. 1 (1996): 293-297. https://doi.org/10.1109/19.481350

[32] Li, Yun Wei, and Jinwei He. "Distribution system harmonic compensation methods: An overview of DG-interfacing inverters." *IEEE industrial electronics magazine* 8, no. 4 (2014): 18-31. https://doi.org/10.1109/MIE.2013.2295421

[33] Kim, S., Gwonjong Yoo, and Jinsoo Song. "A bifunctional utility connected photovoltaic system with power factor correction and UPS facility." In *Conference Record of the Twenty Fifth IEEE Photovoltaic Specialists Conference-1996*, pp. 1363-1368. IEEE, 1996. https://doi.org/10.1109/PVSC.1996.564386

[34] Iqbal, Muzammil, Muhammad Jawad, Mujtaba Hussain Jaffery, Saleem Akhtar, Muhammad Nadeem Rafiq, Muhammad Bilal Qureshi, Ali R. Ansari, and Raheel Nawaz. "Neural networks based shunt hybrid active power filter for harmonic elimination." *IEEE Access* 9 (2021): 69913-69925. https://doi.org/10.1109/ACCESS.2021.3077065

[35] Jayachandran, J., and R. Murali Sachithanandam. "Neural network-based control algorithm for DSTATCOM under nonideal source voltage and varying load conditions." *Canadian Journal of Electrical and Computer Engineering* 38, no. 4 (2015): 307-317. https://doi.org/10.1109/CJECE.2015.2464109

[36] Sinha, Shreya, and Ankita Arora. "Comparison of IRPT and ANN based control algorithm for shunt compensation in grid connected systems." In *2021 International Conference on Intelligent Technologies (CONIT)*, pp. 1-5. IEEE, 2021. https://doi.org/10.1109/CONIT51480.2021.9498281

[37] Singh, Bhim, A. Adya, A. P. Mittal, and J. R. P. Gupta. "Neural network based DSTATCOM controller for three-phase, three-wire system." In *2006 International Conference on Power Electronic, Drives and Energy Systems*, pp. 1-6. IEEE, 2006. https://doi.org/10.1109/CONIT51480.2021.9498281

[38] Singh, Rahul, and Alka Singh. "Performance Evaluation of Three-Phase Unified Power Quality Conditioner controlled using SRF." In *2021 4th International Conference on Recent Developments in Control, Automation & Power Engineering (RDCAPE)*, pp. 486-491. IEEE, 2021. https://doi.org/10.1109/RDCAPE52977.2021.9633640

[39] Badoni, Manoj, Alka Singh, Sandeep Pandey, and Bhim Singh. "Fractional-order notch filter for grid-connected solar PV system with power quality improvement." *IEEE Transactions on Industrial Electronics* 69, no. 1 (2021): 429-439. https://doi.org/10.1109/TIE.2021.3051585

[40] Devi, Sanjenbam Chandrakala, Priyank Shah, Sachin Devassy, and Bhim Singh. "Solar PV array integrated UPQC for power quality improvement based on modified GI." In *2020 IEEE 9th Power India International Conference (PIICON)*, pp. 1-6. IEEE, 2020. https://doi.org/10.1109/PIICON49524.2020.9113032

[41] Roy, Suvom, Farheen Chishti, Bhim Singh, and B. K. Panigrahi. "FOFLL Based Synchronization Scheme with LDLMS Control for Solar Fed Microgrid Feeding Hybrid AC/DC Loads." In *2022 IEEE Energy Conversion Congress and Exposition (ECCE)*, pp. 1-8. IEEE, 2022. https://doi.org/10.1109/ECCE50734.2022.9947747